JGR Atmospheres

RESEARCH ARTICLE
10.1029/2019JD032092

Quantifying Regional Surface Energy Responses to Forest Structural Change in Nordic Fennoscandia

Yogesh Kumkar[1,2], **Rasmus Astrup**[1], **Frode Stordal**[2], **and Ryan M. Bright**[1]

[1]Norwegian Institute of Bioeconomy Research, Ås, Norway, [2]Department of Geosciences, University of Oslo, Oslo, Norway

Abstract In a climate model, surface energy and water fluxes of the vegetated ecosystem largely depend on important structural attributes like leaf area index and canopy height. For forests, management can greatly alter these attributes with resulting consequences for the surface albedo, surface roughness, and evapotranspiration. The sensitivity of surface energy and water budgets to alterations in forest structure is relatively unknown in boreal regions, particularly in Nordic Fennoscandia (Norway, Sweden, and Finland), where the forest management footprint is large. Here we perform offline simulations to quantify the sensitivity of surface heat and moisture fluxes to changes in forest composition and structure across daily, seasonal, and annual time scales. For the region on average, it is found that broadleaved deciduous forests cool the surface by 0.16 K annually and 0.3 K in the growing season owed to higher year-round albedo and lower Bowen ratio, yet in some locations the local cooling can be as much as 2.4 K and 3.0 K, respectively. Moreover, fully developed forests cool the surface by 0.04 K annually in our domain owed to higher evapotranspiration, reaching up to 0.4 K locally in some locations, whereas undeveloped forests warm annually by 0.14 K owed to much lower evapotranspiration reaching up to 0.8 K for some locations. If regional forests are ever to be managed for the local climate regulation services that they provide, our results are an important first step illuminating the potential adverse impacts or benefits across space and time.

Key Points:
- Broadleaved deciduous forests cool annual LST by 0.16 K in Fennoscandia owed to higher surface albedo, ground heat, and lower Bowen ratio
- Undeveloped forests would warm annual LST by 0.14 K, whereas more fully developed forests would cool it by 0.04 K in Nordic Fennoscandia
- Differences in ground heat flux cannot be overlooked when assessing forest management policies aimed at replacing evergreen with deciduous

Supporting Information:
- Figure S1
- Figure S2

Correspondence to:
Y. Kumkar,
yogesh.kumkar@nibio.no

Citation:
Kumkar, Y., Astrup, R., Stordal, F., & Bright, R. M. (2020). Quantifying regional surface energy responses to forest structural change in Nordic Fennoscandia. *Journal of Geophysical Research: Atmospheres*, *125*, e2019JD032092. https://doi.org/10.1029/2019JD032092

Received 20 NOV 2019
Accepted 14 JUL 2020
Accepted article online 16 JUL 2020

Author Contributions:
Conceptualization: Rasmus Astrup, Ryan M. Bright
Data curation: Yogesh Kumkar
Formal analysis: Frode Stordal, Ryan M. Bright
Funding acquisition: Ryan M. Bright
Methodology: Yogesh Kumkar
Project administration: Ryan M. Bright
Supervision: Rasmus Astrup, Frode Stordal, Ryan M. Bright
(continued)

1. Introduction

Forests play an important role in the exchange of mass, momentum, and energy with the atmosphere (Anderson et al., 2011; Bonan, 2008). Forests are considered important to the mitigation of climate change given their carbon sink value, but their biogeophysical properties enhance or suppress the carbon sink benefits depending on their location (Betts et al., 2007). Annually, tropical forests tend to cool the surface locally via large amounts of evapotranspiration (Li et al., 2015; da Rocha et al., 2004), while in temperate forests the dominant annual biogeophysical mechanism is unclear (Anderson et al., 2011; Bonan, 2008; Burakowski et al., 2018; Jackson et al., 2008). Boreal forests tend to warm the surface locally because of their snow masking effect and hence low surface albedos in late winter and early spring (Anderson et al., 2011; Betts, 2000; Bonan, 1993; Li et al., 2015). However, recent observational insight suggests that the strength of the snow masking is highly sensitive to forest structure (Bright et al., 2018), which may deviate significantly between unmanaged and managed portions of the boreal forest zones.

Forest management affects both the species composition and aboveground structure of the forested landscape. Structural attributes like leaf area index (LAI), crown length, and canopy heights are important determinants of surface albedo, evapotranspiration, and surface roughness and thus serve as controls over surface energy, moisture, and momentum fluxes. Land surface models (LSMs) usually classify vegetation into plant functional types (PFTs), within which all parameters are identical, thus ignoring the structural diversity of forests within a simulation grid. Although latest developments in modeling, e.g., the Functionally Assembled Terrestrial Ecosystem Simulator (FATES) in Community Land Model version 5.0 (CLM 5.0; Fisher et al., 2015; Lawrence et al., 2019), can represent forest age classes, many LSMs (e.g., Community Land Model version 4.5 [CLM 4.5]) lack the representation of secondary forests (different development classes analogous to forest management) while calculating the local/regional surface energy budgets; these calculations can be improved by representing the "managed forests" properly in these models (Sato et al., 2015). Recent regional modeling studies (Ahlswede & Thomas, 2017; Luyssaert et al., 2018; Naudts et al., 2016) suggest that management-induced changes to forest structure can be important for the regional surface energy balance because forest management changes the forest structure, which affects the energy

Visualization: Yogesh Kumkar
Writing - original draft: Yogesh Kumkar, Ryan M. Bright
Writing – review & editing: Frode Stordal, Ryan M. Bright

and water vapor exchanges with the overlying atmosphere. Further, Schultz et al. (2016) modified the default configuration of CLM 4.5 so that each PFT is assigned its own soil column and found that the magnitude and patterns of simulated surface air temperature between grass and tree PFT agree closely with the observations than in PFTs' shared soil column setting.

Even though boreal regions like Nordic Fennoscandia have intensively managed forests, management-induced impacts to surface energy and water fluxes have been subjected to little study with LMSs. Empirical studies in boreal regions show that boreal forests have strong warming in winter and cooling in summer with a net annual warming (Alkama & Cescatti, 2016; Li et al., 2015; Zhao & Jackson, 2014). The local surface temperature response to a land management change is found to be of similar order to the response to a land cover change but remains largely unknown (Luyssaert et al., 2014). The estimation of energy and water budgets at land surface is important for determining vegetation's influence on local weather and climate and the study of land-atmosphere dynamics. Numerical models are often used to calculate energy and water budgets at the surface irrespective of the different types of landscapes. The LMSs are capable of isolating the effects of land cover change and land management change as a driver in order to simulate the surface energy and water fluxes across larger spatial scales, which is otherwise not feasible with empirical studies using micrometeorological observations. A recent coupled simulation for Europe shows that historical forest management did not mitigate climate warming although for Nordic Fennoscandia the biogeophysical impact from perturbed surface energy and moisture budgets was less clear (Naudts et al., 2016).

The studies by Naudts et al. (2016) and Luyssaert et al. (2018) prescribe forest management treatments explicitly throughout the domain. Here rather than prescribe forest management treatments, explicitly, we prescribe structural changes as proxies for forest management. This affords certain advantages, such as being computationally more efficient (cheaper), being relatively easier to model, and having fewer computational errors. Further, we perform our study offline (uncoupled with an atmosphere model) as it allows us to maintain a fine resolution at low expense. Considering the complex topography of our domain, fine-resolution models may be better suited to capture steep gradients in forest structure, forest species composition, and leaf area phenology to which surface fluxes are sensitive. Moreover, offline settings are often sufficient to test the hypothesis that structural attributes of forests are important biogeophysical controls over surface energy, water, and momentum fluxes (Alibakhshi et al., 2020; Bohn et al., 2018; Chen & Dirmeyer, 2016, 2020; Laguë et al., 2019; Schulz & Vogel, 2020), which is at the core of this study. We exploit these advantages knowing that atmospheric feedbacks are likely negligible relative to the first order and direct response by surface fluxes at the scale and pattern of regional forestry activities (Chen & Dirmeyer, 2020; Laguë et al., 2019).

The overall aim is to bridge the gap between the forestry science community and climate modeling community and shed new light on the sensitivity of the surface energy balance to structural perturbations in Nordic Fennoscandic boreal forests. The main study objectives are as follows: (1) to quantitatively assess, across time and space, the sensitivity of surface fluxes and land surface temperature (LST) to realistically scaled (i.e., observationally constrained) changes to forest structure and composition; (2) to assess the relative importance of surface energy flux changes to local surface temperature change, and (3) to identify management strategies leading to desirable surface energy balance outcomes.

2. Materials and Methods

2.1. Land Model and Atmospheric Forcing Data

We used CLM4.5 (a land component of the Community Earth System Model) with a domain centered over Nordic Fennoscandia (Norway, Sweden, and Finland) at a horizontal resolution of 4 km × 4 km. Here an "active" land and river transport model with "data" atmosphere (DATM) and "stub" ocean, sea ice, and wave models in offline settings are configured with the observed atmospheric forcing data set version 7 from Climate Research Unit - National Center for Environmental Prediction (CRU-NCEP) (Oleson et al., 2013) in a "satellite phenology" (SP) mode. In SP mode, the model is forced using vegetation phenological climatology, which is derived from satellite data, e.g., Moderate Resolution Imaging Spectroradiometer. An exception, however, is made for forest PFTs where all aboveground structure and monthly phenology are prescribed (section 2.2). All the grid cells within 0.5° receive the same atmospheric forcing. CLM simulates the exchange of energy, water, and momentum between the land surface and the atmosphere using

Table 1
Structural Attributes of Two PFTs and Species Composition

PFT	Species	Structural attributes	Development class (DC) 1	2	3	4
NET	Pine (*Pinus sylvestris*)	H_L	7.5	12.3	16.8	22
		CL	6.3	10.1	13.2	15.8
		LAI_{MAX}	1.4	4.3	6.7	9.1
	Spruce (*Pinus abies*)	H_L	7.5	11.6	17	17.2
		CL	4.6	6.7	9.4	8.4
		LAI_{MAX}	0.9	2.4	2.3	4.4
BDT	Birch dominant (*Betula* spp.)	H_L	4.9	8.4	12.2	18.3
		CL	3.2	5.5	7.9	10.3
		LAI_{MAX}	0.5	1.8	3.9	7

Note. H_L is Lorey's height, CL is crown length, and LAI_{max} is maximum growing season LAI.

process-based submodels of surface energy balance, radiative transfer, hydrology, and vegetation phenology. The simulated fluxes are sent to DATM at every half-hourly time step. The required input variables from DATM via a central coupler are received back, and simulations are performed using a constant CO_2 concentration fixed at the present day (the year 2000). In each grid cell, five land cover types are represented at the subgrid scale. In the vegetated portion of a grid cell, a maximum of 15 PFTs along with their relative fractions are used per soil column as tiles. The albedo (α) of forests depends on the PFT and the time of the year. In CLM, a two-stream radiative transfer scheme is employed for albedo calculations (Oleson et al., 2013) where optical properties of the canopy are fixed for each PFT in the model. Albedo for a vegetated portion of a pixel is a mixture of soil, snow, and vegetation albedo computed separately for visible and near-infrared wavebands and direct and diffuse radiation. In this study, the fractions of either land cover or any PFT within the vegetated land unit are kept unaltered (Figure S1 in the supporting information). Only structural attributes of two PFTs of interest (i.e., needle-leaved evergreen tree [NET] and broadleaved deciduous tree [BDT]) are altered in the representation of forest management.

LST is a good measure of the composite biogeophysical properties affecting the surface energy balance. In this study, we employed energy budget decomposition analysis (given in section 2.4) to quantify the net effect of dynamic responses from a change to forest structural properties.

2.2. Representation of Forest Management Proxies and Data Preparation

The input surface data sets for all experiments (given in the next subsection) are prepared at a horizontal resolution of 0.04° (~4 km) over the spatial domain of Nordic Fennoscandia (mainland Norway, Sweden, and Finland) using default Moderate Resolution Imaging Spectroradiometer (e.g., LAI at 3″ resolution) data and other raw data sets (domain files, grid files, land fraction, glacier, LAI, land water, soil properties, topography, PFT vegetation type, and urban data sets) available at the National Center for Atmospheric Research web server (https://svn-ccsm-inputdata.cgd.ucar.edu/trunk/inputdata/). Here land and PFT cover fractions within the vegetated land unit remain fixed across the three scenarios, and only the four structural parameters LAI, stem area index (SAI), canopy top height (z_{top}), and canopy bottom height (z_{bottom}) are altered. Using national forest inventory information, Majasalmi et al. (2018) recently enhanced the 2015 forest classification of the European Space Agency's Land Cover product (ESA's CCI-LC) for Fennoscandia. The classification differentiates between dominant tree genera or phenology and between forest development stages. For each class, a look-up table provides the following key structural attributes: LAI_{MAX} (m^2 m^{-2}), crown length (m), and Lorey's height (m). These are summarized in Table 1 for the reader's convenience.

Here we make use of the look-up table to prescribe a "present state of forest," or control forest management scenario (PRESENT), representing the current structure and compositional state of regional forests. Three alternate management scenarios are designed to span the full range of compositional and structural changes potentially affected by management activities. Briefly, the first scenario, or "All Development Class 1 (DC1)," represents undeveloped forests; the second scenario, or "All Development Class 4 (DC4)," represents highly developed forests; and the third scenario, or "Broadleaved Deciduous PFT Class 4 (BDT4)," represents highly developed and all-deciduous broadleaved forests. In DC1, structural attributes of PRESENT are changed to those of the least developed class (i.e., lowest LAIs and canopy heights) and species compositions remain unaffected, whereas in DC4, the structural attributes of PRESENT are changed to those of the most developed class (i.e. highest LAIs and canopy heights) with species compositions unaffected. In BDT4, all evergreen needleaved species in PRESENT are changed to those of BDT and structural attributes are changed to those of the most developed class The equations to prepare PRESENT and three alternate scenarios are given in Table S1 of the supporting information.

Prescribing low LAIs and canopy heights in the All DC1 scenario does in essence account for the effect of clear-cut harvesting, with the implemented changes being fully constrained by observations. In All DC4, although not constrained by observation, the prescribed structural changes are meant to capture a broad

range of management interventions that could potentially enhance stand volume densities in the future, such as more optimal planting densities, precommercial thinning regimes, and fertilization. In All DC4, the prescribed LAI and canopy heights correspond to the most developed classes of Majasalmi et al. (2018).

The spruce and pine classes of Majasalmi et al. (2018) are considered as a NET PFT, while the deciduous class is considered as a BDT PFT. We computed monthly LAI phenology for BDT using the budburst model of Olsson and Jönsson (2014), senescence model from Dixon (1976), and daily near-surface air temperature from Lussana et al. (2018). The NET LAI phenology is negligible, and thus, monthly LAI is set to LAI_{MAX}. Area weighted mean annual LAI of PRESENT, DC1, DC4, and BDT4 are presented in the supporting information along with their differences from PRESENT (cf. Figures S2a–S2c and S3–S6). BDT SAI, defined here as the one-sided branch area plus the one-sided area of dead foliage, is a function of LAI and is based on the prognostic model of Zeng et al. (2002). BDT SAI is set to the default value in CLM (i.e., 1) in the first time step, which is taken here as the month of July. For NET, the default CLM value of 1 is used for all months.

2.3. Experimental Setup

Two pairs of experiments are set up to assess the sensitivity of surface fluxes to important environmental background controls (temperature and precipitation) and to modeling assumptions about PFT competition for soil moisture. For the former, we analyzed historical trends in vapor pressure deficit (VPD) during the growing season within our study domain and identify two anomalous years—one with high and one with low VPD (see Figure S7 in the supporting information), which we term "DRY" and "WET," respectively. For the latter, we carry out simulations when all PFTs share a common soil column and when they are given their own separate soil columns (SSCs) as in Schultz et al. (2016). This results in the four experiments shown in Table S2 in the supporting information. Given the importance of assigning each PFT its own soil column, we emphasize experiment SSC throughout this study at additional negligible computational costs and model code modifications.

The initial condition is prepared by spinning up the model for 31 years in order for the system to reach a dynamic equilibrium. Since all the experiments are carried out in SP mode, 30 years of spin-up is found to be sufficient after analyzing the soil moisture data (after 25 years, the variability in soil moisture data ceases). All simulations are made from a common initial state, but each is run with different land surface input data, reflecting the three forest management scenarios. We analyzed only NET and BDT PFTs, discarding all others including bare ground.

2.4. Surface Energy Balance Metrics and Decomposition

The surface energy balance is governed by biogeophysical properties of the surface that affect the surface albedo, ground heat conductance, and partitioning of turbulent heat fluxes. The LST is an important indicator of the local climate derived here from emitted longwave radiation using the Stefan–Boltzmann law as given in Oleson et al. (2013). The attribution of differences in simulated LST between one of our three management scenarios and PRESENT—or (ΔLST)—to the differences in the surface fluxes and albedo is helpful for understanding the most important drivers. From here on, Δ is used for the differences in simulated variable between one of the three scenarios and PRESENT. Several techniques have been developed to access the relative importance of individual surface energy balance terms or mechanisms controlling LST such as the intrinsic biophysical mechanism (Lee et al., 2011), the temperature decomposition method (TDM) (Luyssaert et al., 2014), and the two-resistance method (Rigden & Li, 2017). The intrinsic biophysical mechanism and two-resistance method attribute ΔLST to changes to mechanisms, while TDM attributes ΔLST to changes to fluxes and albedo (Winckler et al., 2019). Here we apply TDM to attribute ΔLST to differences in surface fluxes and albedo (α) (Luyssaert et al., 2014) with a slight modification:

$$\Delta \mathrm{LST}^{\mathrm{TDM}} \approx \frac{-S\downarrow \Delta\alpha - \Delta H - \Delta\lambda Ev - \Delta\lambda Tr - \Delta G}{4\varepsilon\sigma T_s^3} \tag{1}$$

where $-S\downarrow\Delta\alpha/4\varepsilon\sigma T_s^3$ is the ΔLST from the change to the surface albedo, $-\Delta H/4\varepsilon\sigma T_s^3$ is the ΔLST from the change to the sensible heat, $-\Delta G/4\varepsilon\sigma T_s^3$ is the ΔLST due to the change to the ground heat flux (G), and the ΔLST from the change to the latent heat flux (LE) is decomposed into the contribution from the change in total evaporation $-\Delta\lambda Ev/4\varepsilon\sigma T_s^3$ (sum of canopy evaporation [E_c] and surface evaporation

[E_s]) and transpiration (Tr) $-\boldsymbol{\Delta\lambda Tr/4\varepsilon\sigma T_s^3}$ (where λ is the latent heat of vaporization). Note that other terms of TDM of Luyssaert et al. (2014) such as $\Delta S\downarrow$ (incoming shortwave radiation) and $\Delta L\downarrow$ (incoming longwave radiation) are excluded because of the decoupling with the atmosphere. ΔLST from $\Delta\varepsilon$ (emissivity) is assumed negligible (Juang et al., 2007) and is also excluded from the temperature decomposition, although the effect of this assumption is assessed as the difference of $\Delta LST^{TDM} - \Delta LST$.

For each simulation, we obtained all fluxes at the PFT level (per square meter in a grid cell) but present them here at the grid level by weighting them by the total forest PFT area within each grid cell. The maps in all figures including the supporting information thus indicate the local effect of each 4 km grid cell (as opposed to per square meter within the grid cell).

3. Results

Results are presented as differences between the three management scenarios and the control (PRESENT), i.e., "DC1-PRESENT," "DC4-PRESENT," and "BDT4-PRESENT." Changes in input structure associated with each scenario are presented in Figures S3–S6 in the supporting information. Using summertime (June-July-August) Bowen ratio differences ($\Delta\beta$) as a measure, we find that differences in the representation of subgrid hydrology are relatively uniform spatially across scenarios (Figure S8). Regarding the atmospheric forcing (WET, or low VPD, vs. DRY, or high VPD, years), differences in the spatial pattern of $\Delta\beta$ across scenarios are more apparent (Figure S9). However, we choose to limit the presentation of all results henceforth to those of Experiment 3 "SSC-WET" (Table S2) because giving forest PFTs their own SSCs has been shown to improve accuracy in the modeling of surface fluxes in other regions (Meier et al., 2018; Schultz et al., 2016) and because the WET year (2012 VPD)—although the wettest within our 8 year atmospheric forcing data set—aligned more closely with the longer-term mean for the period spanning 1979–2017 (Figure S7, top).

3.1. Turbulent Heat Flux Partitioning and Evapotranspiration

Starting with DC1-PRESENT and summer, although the mean $\Delta\beta$ for the entire domain is 0.19 (Table 2), it can be as high as 1.2 in the southernmost portions where large reductions in canopy transpiration and canopy evaporation offsets the increases to soil evaporation (Figures 1d, 1g, and 1j). For DC4-PRESENT and BDT4-PRESENT, the mean $\Delta\beta$ for the entire domain is −0.11 and −0.15 (Table 2), respectively. It is as low as −1.26 in southernmost regions of the domain where large reductions in soil evaporation offsets the increases in canopy evaporation and transpiration in DC4-PRESENT. Although the mean $\boldsymbol{\Delta\lambda ET}$ for the entire domain in BDT4-PRESENT is of similar order as that of DC4-PRESENT, the reductions in canopy evaporation and transpiration offsets soil evaporation along the western and northern portions of the domain.

Interestingly, despite differences in the changes imposed to forest structure between DC4-PRESENT and BDT4-PRESENT (Figures S3–S6), the summertime spatial patterns and magnitudes in $\Delta\beta$ are almost identical, but patterns in the three moisture fluxes differ. In BDT4-PRESENT, for instance, LAI is increased, while z_{top} is decreased (Figure S1), increasing dry and wet canopy conductances but decreasing aerodynamic conductance such that the magnitude of the net moisture flux change resembles that of DC4-PRESENT.

Over the annual time scale and for the full domain, the mean $\Delta\beta$ is −0.44, −0.89, and −3.34 for DC1-PRESENT, DC4-PRESENT, and BDT4-PRESENT, respectively (Table 2). In DC1-PRESENT, the annual regional mean $\Delta\beta$ is attributed mostly to decreases in latent heat (−1.82 W/m^2) rather than to increases in sensible heat (0.80 W/m^2). For DC4-PRESENT, the annual regional mean $\Delta\beta$ is attributed more to increases to latent heat (1.48 W/m^2) rather than to decreases in sensible heat (−1.33 W/m^2). In BDT4-PRESENT, however, the annual regional mean $\Delta\beta$ is attributed mostly to decreases to sensible heat (−4.0 W/m^2) rather than to increases to latent heat (1.2 W/m^2).

3.2. Albedo

For all scenarios, the largest $\Delta\alpha$ occurs in winter, and for DC1-PRESENT and DC4-PRESENT, it is mostly confined to the central and eastern portions of the study domain (Figure 2) where air temperatures are lower and where canopy snow masking effects driven by ΔLAI are greater relative to the warmer western regions. For BDT4-PRESENT in winter, ΔLAI is negative, resulting in a large positive $\Delta\alpha$ in all regions where ΔLAI is imposed. In the other three seasons, spatial patterns of $\Delta\alpha$ are similar between DC1-PRESENT and

Table 2
Regional Summertime (June-July-August) Forest Area-Weighted Averages of the Component Latent Heat Fluxes ($W\ m^{-2}$) and Bowen Ratios (Unitless) for the Three Scenarios

	Summer average			
Scenario	Bowen ratio ($H/\lambda ET$)	Canopy evaporation (λEv_{canopy})	Transpiration (λTr)	Soil evaporation (λEv_{soil})
DC1-PRESENT	0.19 (0.22)	−2.12 (2.13)	−8.15 (7.86)	5.00 (4.67)
DC4-PRESENT	−0.11 (0.16)	1.38 (1.50)	5.08 (5.39)	−3.20 (3.43)
BDT4-PRESENT	−0.15 (0.17)	1.44 (1.65)	4.73 (5.38)	−2.50 (3.88)
	Annual average			
Scenario	Bowen ratio ($H/\lambda ET$)	Sensible heat (H)	Latent heat (λET)	
DC1-PRESENT	−0.44 (0.2)	0.80 (2.14)	−1.82 (2.51)	
DC4-PRESENT	−0.89 (0.14)	−1.33 (1.80)	1.48 (1.72)	
BDT4-PRESENT	−3.34 (0.22)	−4.02 (2.72)	1.20 (1.89)	

Note. The annual forest area-weighted averages of Bowen ratios and sensible heat and latent heat for three scenarios are shown in last three rows. The numbers in parentheses are standard deviations between a particular scenario and PRESENT.

DC4-PRESENT but opposite in sign. These patterns do not appear to fully align with the spatial patterns in the annual mean ΔLAI (Figure S1), suggesting that $\Delta\alpha$ from canopy (un)masking may be sensitive to regional differences in ground surface albedo. For instance, for DC1-PRESENT in summer and autumn (snow-free periods), we see slight reductions to albedo rather than increases as would be expected from

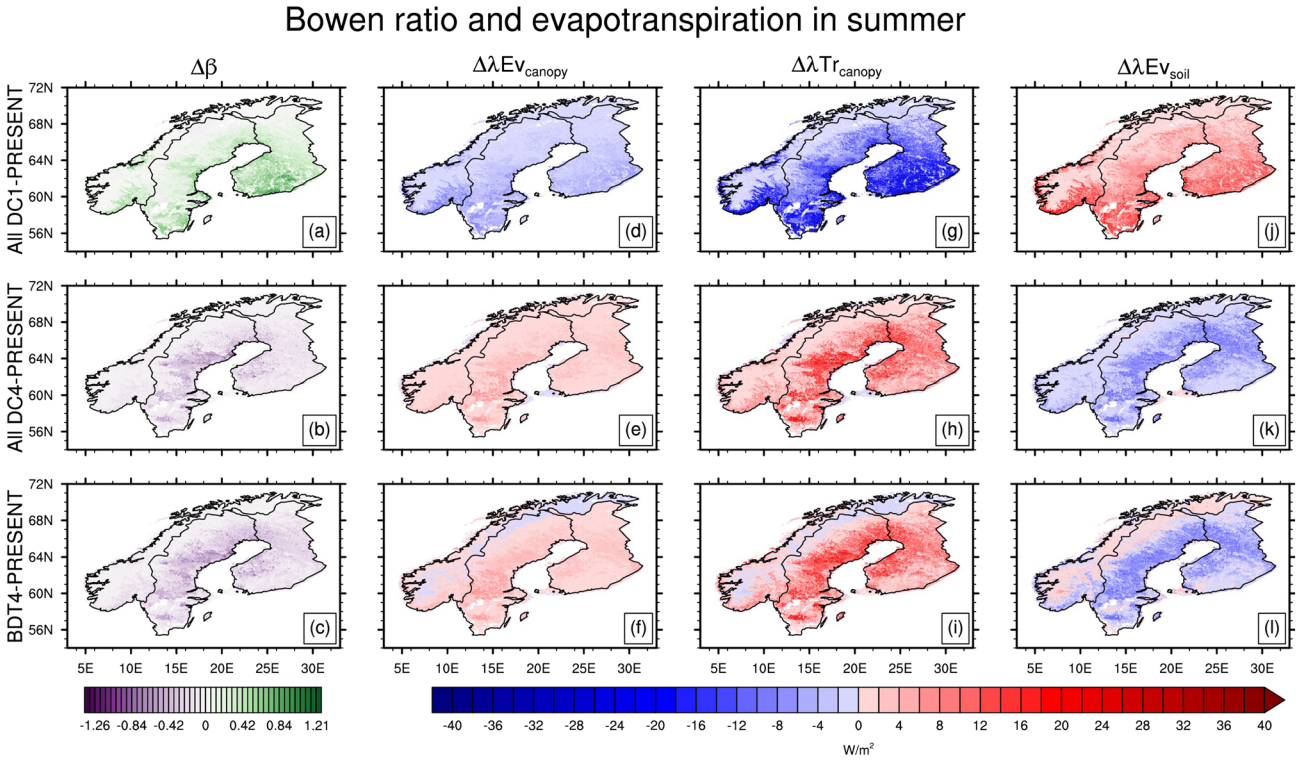

Figure 1. Differences in summertime Bowen ratio ($\Delta\beta$), canopy evaporation ($\Delta\lambda E_{canopy}$), canopy transpiration ($\Delta\lambda T_{canopy}$), and soil evaporation ($\Delta\lambda E_{soil}$) between three scenarios and PRESENT.

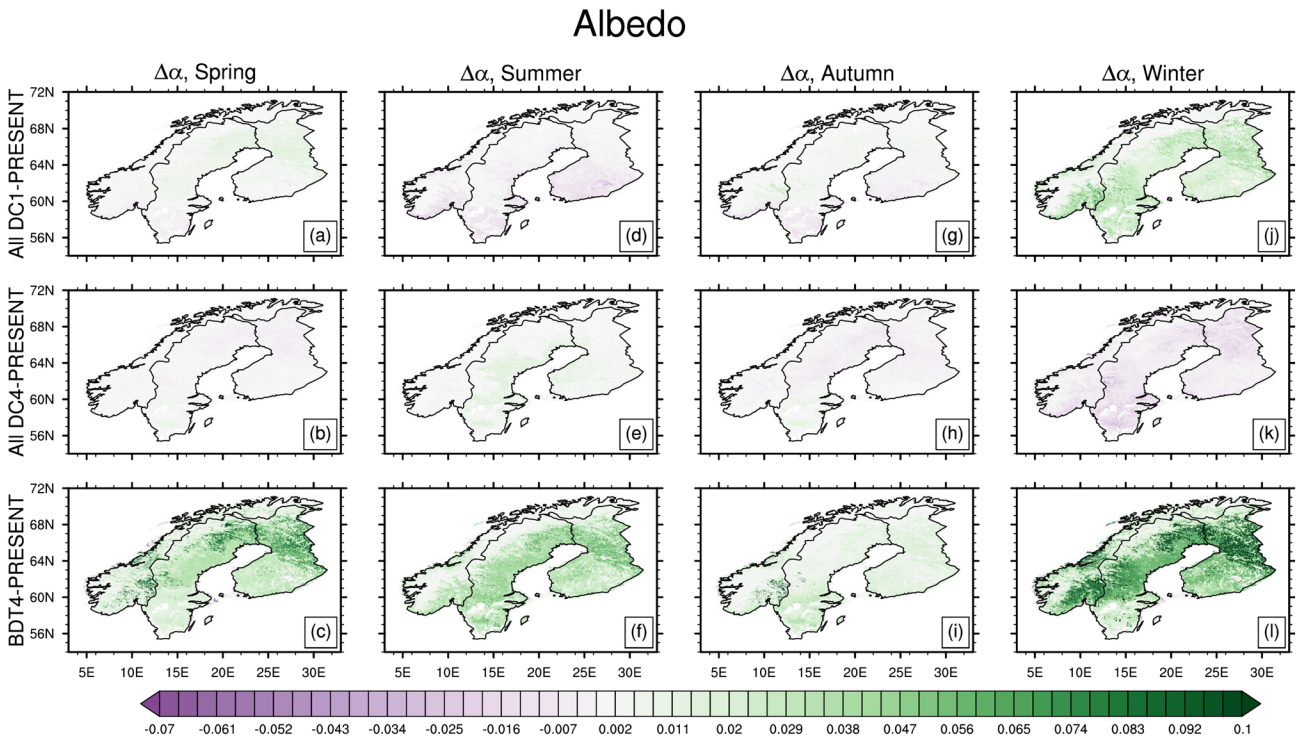

Figure 2. Differences in seasonal mean surface albedo for three alternative forest management scenarios from PRESENT.

reduced canopy masking. An inspection of the CLM soil color map (Figure S10 and Table S3) reveals that soils in the southern portions of our domain have the lowest surface albedo properties relative to the rest of the domain. Given the type of albedo scheme employed in CLM with only one canopy layer and where the soil albedo plays a greater influence on the total surface albedo, this result is to be expected.

Driven by reductions in canopy masking of the ground surface, the difference in regional mean surface albedo ($\Delta\alpha$) in DC1-PRESENT is positive in all seasons except summer and autumn (Table 3) where the regional mean is determined by albedo decreases in the southern portions of our domain (Figure 2, first row). Regional mean $\Delta\alpha$ in DC4-PRESENT is −0.0064 in winter, 0.00007 in spring, 0.0031 in summer, and −0.0008 in autumn (Table 3). Highly developed forests in DC4-PRESENT have higher LAI and taller canopy heights, which serve to enhance the snow masking effect in autumn and winter, resulting in lower surface albedos during these seasons relative to PRESENT.

The largest regional mean $\Delta\alpha$ is found for BDT4-PRESENT, and it is positive in all seasons (Table 3), driven by decreases in canopy masking during winter and autumn and increases in canopy albedo during summer and spring. The annual regional mean $\Delta\alpha$ for DC1-PRESENT, DC4-PRESENT, and BDT4-PRESENT are 0.0041, −0.001, and 0.0271, respectively.

3.3. Ground Heat

Starting with DC1-PRESENT, the mean ΔG for the entire domain is 1.84, −0.04, −0.91, and −0.18 in spring, summer, autumn, and winter, respectively (Table 4). The largest ΔG occurs in spring (up to 9 W m^{-2}) and

Table 3
Regional Seasonal Forest Area-Weighted Averages of Surface Albedo (Unitless) for the Three Scenarios

Scenario	Spring	Summer	Autumn	Winter
DC1-PRESENT	0.0031 (0.01)	−0.0029 (0.01)	0.0002 (0.00)	0.0162 (0.01)
DC4-PRESENT	0.0000 (0.00)	0.0031 (0.01)	−0.0008 (0.00)	−0.0064 (0.01)
BDT4-PRESENT	0.0272 (0.03)	0.0234 (0.02)	0.0107 (0.01)	0.0471 (0.05)

Note. The numbers in the parentheses are standard deviations between a particular scenario and PRESENT.

Table 4
Regional Seasonal Forest Area-Weighted Averages of Ground Heat (Wm^{-2}) for the Three SScenarios

Scenario	Spring	Summer	Autumn	Winter
DC1-PRESENT	1.84	−0.04	−0.91	−0.18
DC4-PRESENT	−1.14	0.25	0.72	0.11
BDT4-PRESENT	3.24	−2.51	0.90	1.30

autumn (up to −4 W m^{-2}), confined mostly to the southern and central portions of the study domain (Figure 3). In summer, ΔG is as low as −8 W m^{-2} in central Sweden and Norway (high-altitude regions) but closer to 1 W m^{-2} in the rest of the domain. In winter, ΔG is about 0.5 W m^{-2} in most of the domain but up to −2 W m^{-2} in southern Sweden, which makes the regional mean −0.16 W m^{-2} for DC1-PRESENT. For DC4-PRESENT, the patterns of ΔG are opposite to that of DC1-PRESENT in all seasons, and the mean ΔG for the entire domain is −1.14, 0.25, 0.72, and 0.11 in spring, summer, autumn, and winter, respectively (Table 4). Here, in spring, ΔG is as low as −10 W m^{-2} in northern Sweden and Finland and as high as 4 W m^{-2} in summer at the same locations. In autumn and winter, it is higher in southern portions of the domain. The seasonal changes in ground heat at these locations are due to seasonal phenological changes in aboveground structure of the deciduous PTF in forests. The mean ΔG for the entire domain is 3.24, −2.51, 0.90, and 1.30 in spring, summer, autumn, and winter, respectively for BDT4-PRESENT (Table 4). This is the largest regional mean ΔG among all scenarios in all seasons, suggesting that ground heat flux plays an important role in surface energy budget in deciduous forests. The magnitude of ΔLAI, Δz_{top}, and Δz_{bottom} in all seasons for all scenarios are of similar orders but with different signs (Figures S2–S6). DC1-PRESENT and DC4-PRESENT consist predominately of NET, whereas in BDT4-PRESENT, only BDT exists. Thus, differences in LAI phenology play a much larger role in BDT4-PRESENT relative to DC1-PRESENT and DC4-PRESENT.

The magnitude of ΔG are of similar orders in all seasons for DC1-PRESENT and DC4-PRESENT, but their signs are opposite, suggesting that ground heat flux is highly sensitive to ΔLAI because the signs of ΔLAI

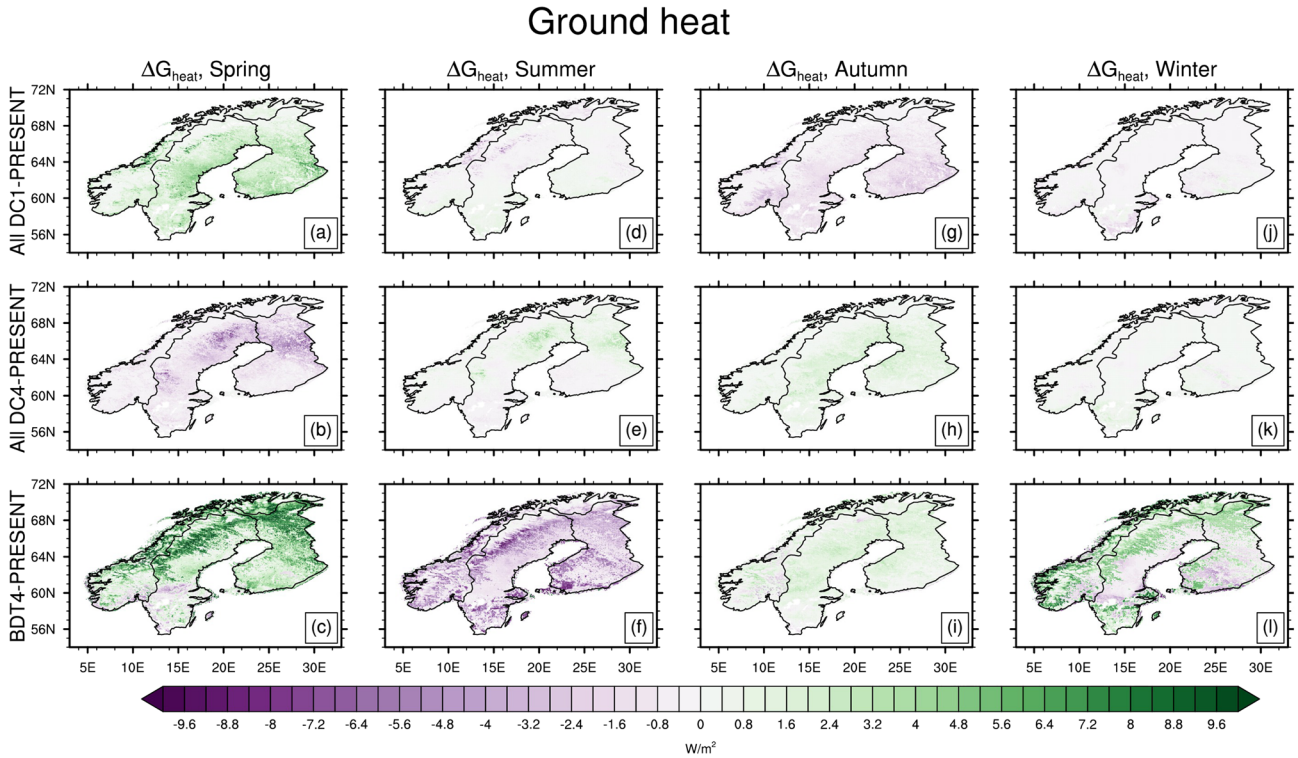

Figure 3. Differences in ground heat between three forest management scenarios and PRESENT in all seasons.

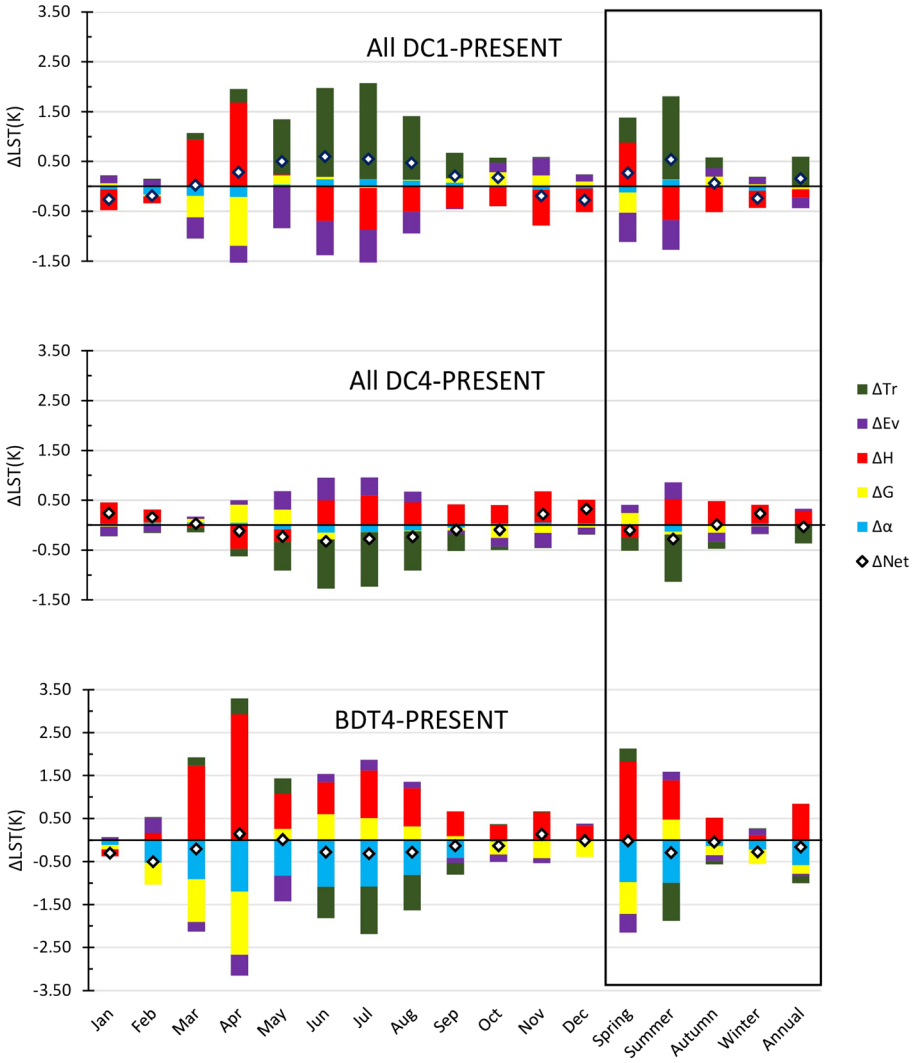

Figure 4. Attribution of ΔLST to Δ*Tr*, Δ*Ev*, Δ*H*, Δ*G*, and Δ*α* based on the temperature decomposition method (TDM). The magnitudes of bars are averages for the entire domain.

are also opposite for those scenarios. Overall, in spring (after snow melt), the Δ*G* is much higher in DC1-PRESENT and BDT4-PRESENT than in DC4-PRESENT (Figure 3), where LAI is relatively lower (Figure S3). This is also true for BDT4-PRESENT in winter, where LAI is least among all scenarios (Figures S6i). Although ΔG for BDT4-PRESENT is large and negative in summer, it is positive in large portions of the domain for the other three seasons, which results in an annual mean of 0.73 W m^{-2} for the entire domain. The annual regional mean Δ*G* for DC1-PRESENT, DC4-PRESENT, and BDT4-PRESENT are 0.179, −0.014, and 0.733, respectively.

3.4. LST and Its Decomposition

Starting with DC1-PRESENT and spring, warming is found throughout most of the domain, with ΔLST reaching up to ~1 K in the southern portions (Figure S12). Spring warming is owed to combined decreases to *H* and λ*Tr*, which outweigh combined increases to *α*, *G*, and λ*Ev* (Figure 4). Even greater warming is found throughout the domain during summer, where ΔLST can extend up to 2 K in the south and 1 K in the rest of the domain's lowland regions (see Figure S11 for topography detail), which is attributed to the large warming owed to reductions to λ*Tr*. As in spring and summer, ΔLST for most of the domain in autumn is positive and around ~ 0.5 K although in this season the warming signal stems from decreases to both λ*Tr* and λ*Ev* as well as from decreases to *G* (Figure 4). A cooling is found for most of the domain during winter, varying from

~ −2 K in eastern Norway to ~ −0.5 K in the far north, far south, and in the higher elevation portions of the domain (Figure S12, fourth column). This cooling is mostly owed to increases in H and α. Annually, ΔLST is mostly positive throughout the domain, dominated largely by decreases to λTr in the south, where it can reach ~1.25 K, and by decreases to H in the north and central higher elevation regions, where it reaches ~0.5 K (Figure 4). For DC1-PRESENT, it appears that reductions to the transpiration flux dominates the annual mean ΔLST signal, with changes to albedo playing a more limited role than anticipated outside winter.

Moving on to DC4-PRESENT, during spring a net and near-uniform cooling of around ~ −0.75 K is found throughout most of the domain, which is mostly owed to increases in λTr in the south and in H in the north of Sweden and Finland (Figure S13). The signal from $\Delta\alpha$ is varied, where a small cooling due to albedo increases is seen in the south despite the increase to forest canopy heights and leaf areas. The finding that canopy masking enhances rather than reduces the surface albedo in these areas suggests that these regions are mostly snow free during spring and that the albedo of ground and understory is lower than the albedo of forest canopies. A close inspection of the map of soil albedos (Figure S10) reveals that the darkest soils are found in the southern portions of Norway, Finland, and Sweden, suggesting that this indeed might be the case.

Opposite of DC1-PRESENT, the net ΔLST in spring here is owed to the combined increases in H and λTr, which outweigh the combined decreases to α, G, and λEv. Even greater net cooling is found throughout the domain during summer, where ΔLST can extend up to ~ −1.5 K in western Finland and in the lowland areas of southern and central Sweden (Figure S13). Like in spring, this cooling is mostly owed to $\Delta\lambda Tr$ signal. The net ΔLST is more spatially varied in autumn with no clear pattern, ranging from ~ −0.25 K to ~0.25 K. Where there is net warming, there appears to be a relatively large signal stemming from ΔH (Figure 4). In winter, a net warming is found for the entire domain, approaching ~1 K in the lowland regions of Sweden and central Finland, which appears to be driven more by decreases to H rather than to α (Figure S13). Annually, DC4-PRESENT results in a mean cooling of ~ −0.25 K to −0.5 K for large portions of the domain that appears to be driven mostly by enhancements to transpiration (λTr). In southern and middle Norway, the net annual warming of ~0.25 K appears to mostly be determined by the signal arising from decreases in H, whereas in the other warming areas of the northern and eastern parts of the domain, the warming appears to mostly be determined by the signal arising from the decrease in evaporation (λEv).

Moving on to BDT4-PRESENT, during spring, net ΔLST varies spatially, with moderate warming of ~0.5–1 K occurring throughout the lowland regions of eastern Norway, Sweden, and Finland and a moderate cooling of ~ −1 K to −0.5 K elsewhere (Figure S14). Where there is a net warming, we find that the largest signal is from ΔH, whereas increases to both α and G give the largest cooling signals in regions where we find net cooling (Figure 4). In summer, the net ΔLST spatial pattern appears inverted from spring, with strong cooling of ~ −2 K occurring throughout the lowland regions of eastern Norway, Sweden, and Finland, and a moderate warming of ~1 K elsewhere. In summer, this strong cooling is owed largely to increases to surface albedo, whereas the combined effects of changes to G and λTr dominate the signal for the locations with warming (Figure 4). In autumn, a net moderate cooling is found for most of the domain with the exception of eastern central Sweden, where a moderate warming is evident. In winter, a mild net warming is found in southern Sweden and Finland, which appears to be dominated by reductions to both the sensible (H) and latent (λE and $\Delta\lambda Tr$) heat fluxes offsetting signals from ΔG and $\Delta\alpha$ (Figure S14). Elsewhere a moderate to strong cooling is found where ΔG and $\Delta\alpha$ are the dominant signals. Annually, a moderate cooling of around −0.75 K to −1 K is found throughout most of the domain, which is largely owed to increases in albedo in each season (Figure 4).

As for regional seasonal means, starting with summer the net ΔLST is 0.50 K, −0.28 K, and −0.30 K, respectively, for DC1-PRESENT, DC4-PRESENT, and BDT4-PRESENT (Figure 4). $\Delta\lambda Tr$ (changes to latent heat of canopy transpiration) dominates ΔLST in DC1-PRESENT and DC4-PRESENT (Figure 4), whereas in BDT4-PRESENT $\Delta\alpha$ (change in surface albedo) is the dominant signal. In winter, the regional mean net ΔLST is −0.22 K, 0.22 K, and −0.26 K for DC1-PRESENT, DC4-PRESENT, and BDT4-PRESENT, respectively (Figure 4). ΔH (sensible heat) dominates ΔLST in Scenarios 1 and 2, whereas in BDT4-PRESENT ΔG (change in ground heat flux) is the dominant signal (Figure 4). For the latter, a rapid increase in broadleaf deciduous LAI following budburst in May prevents ΔG from becoming the dominant cooling signal also

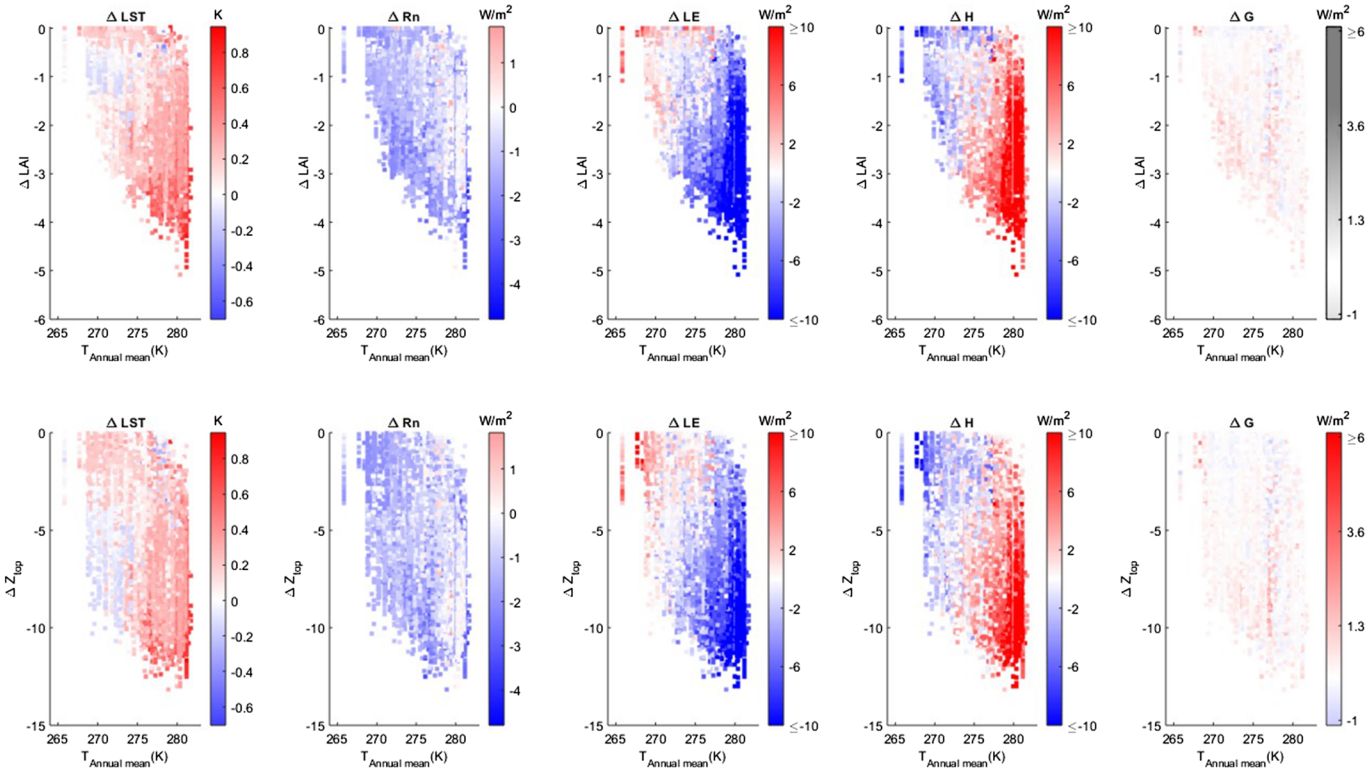

Figure 5. Interplay between ΔLAI and ΔLST, Δ*Rn*, ΔLE, Δ*H*, Δ*G* (first row) across mean annual temperature gradient in Nordic Fennoscandia for DC1-PRESENT. Interplay between Δz_{top} and ΔLST, Δ*Rn*, ΔLE, Δ*H*, and Δ*G* (second row) across mean annual temperature gradient in Nordic Fennoscandia for DC1-PRESENT.

in spring. Here, and also for summer, the dominant cooling signal in BDT4-PRESENT appears to stem from Δα.

The regional annual mean ΔLST is 0.14 K, −0.04 K, and −0.16 K in DC1-PRESENT, DC4-PRESENT, and BDT4-PRESENT, respectively (Figure 4). At the annual time scale, Δ*Tr* dominates ΔLST in both DC1-PRESENT and DC4-PRESENT (warming and cooling, respectively), whereas in BDT4-PRESENT Δ*H* dominates. Although Δ*H* is the dominant annual mean ΔLST signal in BDT4-PRESENT, the collective cooling signals from Δα, Δ*Tr*, and Δ*G* dictate the sign of the annual ΔLST response.

Although at the regional level the net annual ΔLST is negative in BDT4-PRESENT, a positive annual ΔLST is found in southern Finland, in southern Sweden, and in western north Norway (Figure S14). These are regions where Δα and Δλ*Tr* are lowest.

As for the neglected Δε, we infer this to be 0.014, 0.0005, and 0.002 annually for the three scenarios (the difference between ΔLST reconstructed with Equation 1 and the simulated ΔLST).

3.5. Sensitivity of Surface Fluxes to Structural Change and Background Climate

The sensitivity of surface fluxes to forest structural change in Nordic Fennoscandia can be appreciated when looking at Figure 5 for DC1-PRESENT (no species change, ΔSpecies = 0). Figures 5 and 6 show that the magnitude of the annual LST response tends to scale with the magnitude of decreases to LAI (negative ΔLAI) and canopy top heights (z_{top}). However, the sign of ΔLST appears to be sensitive to a limited range of ΔLAI and Δz_{top} below mean annual temperature and precipitation thresholds of 275 K and 1,000 mm, respectively. Although decreases in LAI generally reduce *Rn* via increases to surface albedo, negative Bowen ratio changes (i.e., negative Δ*H* and positive ΔLE) appear to revert to positive Bowen ratio changes (i.e., positive Δ*H* and negative ΔLE) around 275 K (Figure 5, seasonal mean climate is shown in Figures S15 and S16) and 1,000 mm (Figure 6). These could be climate thresholds below which transpiration (*Tr*) dominates the surface moisture flux, which, given the finding reported in Launiainen et al. (2016) about

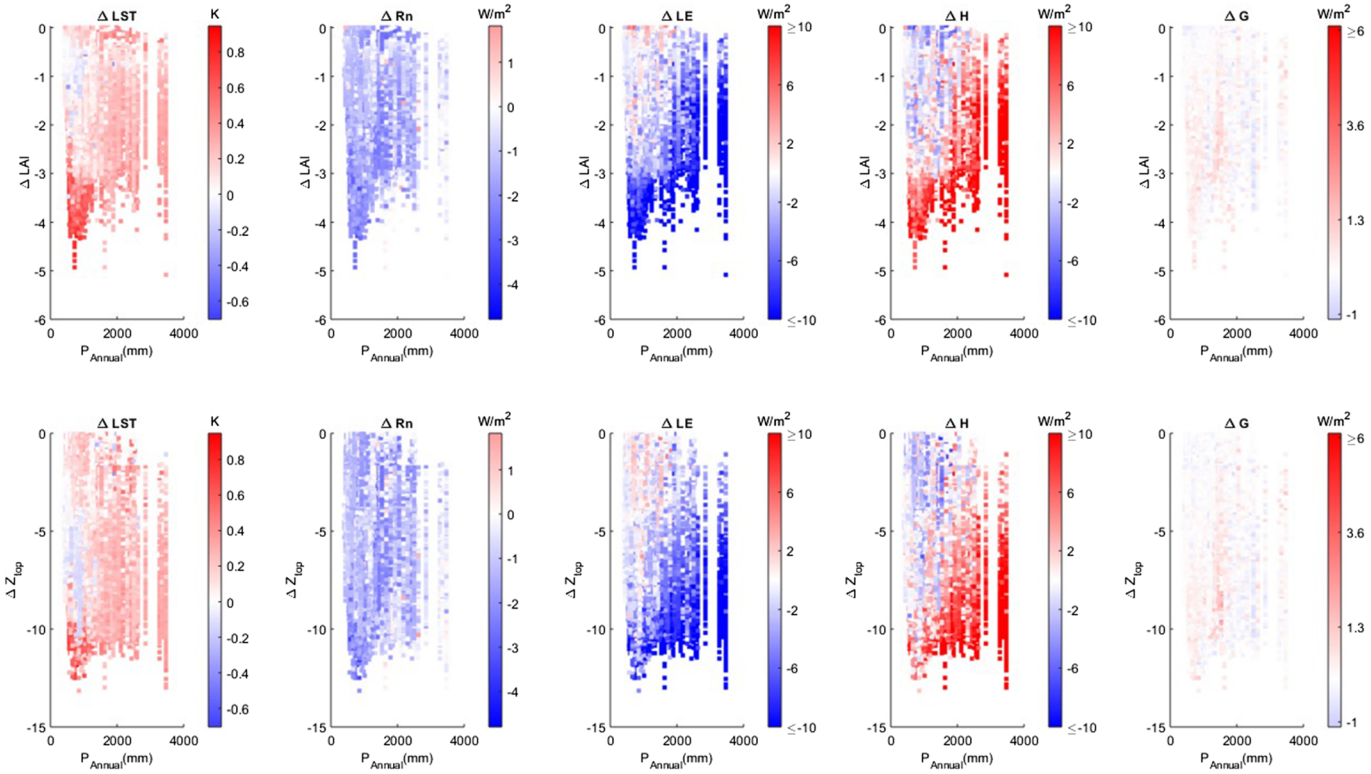

Figure 6. Interplay between ΔLAI and ΔLST, Δ*Rn*, ΔLE, Δ*H*, Δ*G* (first row) across annual precipitation gradient in Nordic Fennoscandia for DC1-PRESENT. Interplay between Δz_{top} and ΔLST, Δ*Rn*, ΔLE, Δ*H*, Δ*G* (second row) across annual precipitation gradient in Nordic Fennoscandia for DC1-PRESENT.

dry canopy conductance minima between 0.5 and 1.5 LAI in Swedish and Finnish boreal forests having similar climate backgrounds, could explain why we find a surface cooling between the ΔLAI range of −0.5 to −2 m^2 m^{-2}.

4. Discussion

The first objective of this study was to quantitatively assess the sensitivity of the surface energy and moisture balances to hypothetical forest management (forest structure as proxies of forest management) change in Nordic Fennoscandia in space and time. We addressed it by analyzing seasonal changes in simulated Bowen ratio, ground heat flux, surface albedo, evapotranspiration, and surface temperature to changes to canopy heights (z_{top} and z_{bottom}), LAIs, and dominant tree species as constrained by regional observations. Changes to annual and regional mean Bowen ratios ($\Delta\beta$) were greater in magnitude for a simulation mimicking the conversion of the present-day forest state (PRESENT) to least developed forests than for a simulation mimicking the opposite (i.e., the conversion of PRESENT to fully developed forests). The magnitude of the annual $\Delta\beta$ for a simulation mimicking the conversion of existing, predominantly coniferous forests to deciduous forests fell in between the "fully developed" and "undeveloped" conversion scenarios. The sensitivity of $\Delta\beta$ to ΔLAI, Δz_{top}, and ΔSpecies appeared (e.g., Figures 5 and 6) to be in line with that distilled from observations at paired FLUXNET sites in other boreal forest regions (e.g., Beringer et al., 2005; Chambers, 2005; Eugster et al., 2000; Huang et al., 2013; Liu & Randerson, 2008), giving confidence in our modeling results (Table S4).

The regional mean $\Delta\alpha$ from the conversion of PRESENT to deciduous forests was higher than that for the conversion of PRESENT to either undeveloped or fully developed forests in all seasons, with an annual mean $\Delta\alpha$ that was found to be 1 order of magnitude larger than the regional annual mean $\Delta\alpha$ for the two scenarios with no species and only structural changes. The sensitivity of surface albedo in the region to changes to ΔLAI, Δz_{top}, and ΔSpecies is in line with both observational (Bright et al., 2015; Hovi et al., 2016; Kuusinen et al., 2016) and forest reflectance modeling studies (Lukeš et al., 2013). Further, our $\Delta\alpha$ results

of All DC4 and BDT4 in the growing season align with the albedo results (Figure 4 of Alibakhshi et al., 2020) in boreal regions.

The conversion of PRESENT to deciduous forests resulted in a much higher annual ΔG than the conversion to undeveloped and fully developed forests (Figure 3), which we suspected initially could have been attributed to differences in leaf area phenology between NET and BDT. However, after further inspection, we found little correlation between the imposed differences in LAI and ΔG (Figure S17), suggesting that differences in G between BDT and NET might be attributed instead to differences in belowground vegetation structure and/or to tree physiology. For instance, the BDT PFT in CLM is parameterized to have substantially greater rooting depths and a different tree hydraulic architecture than NET (Meier et al., 2018; Schultz et al., 2016), as well as different leaf stomatal conductance (Oleson et al., 2013), which collectively may be driving different transpiration rates and in turn impacting the soil moisture differently. The thermal conductivity of soils increases with increasing soil moisture, which has the effect of increasing G and reducing surface temperature over a diurnal cycle (Nobel & Geller, 1987). Essentially, we suspect that physiological and belowground structural differences might be affecting the soil moisture regime and hence the soil thermal state, i.e., thermal conductivities and volumetric heat capacities (Oyeyemi et al., 2018), which affects the temperature of the uppermost soil layer. However, because G is estimated as a residual term in the ground surface energy balance equation in CLM and not explicitly linked to any soil parameters or processes, it is not possible to evaluate this hypothesis. Although observational evidence of ΔG in Nordic Fennoscandia is lacking (existing in situ observations are for evergreen needleleaved forests only), results from studies in other regions are comparable. The magnitudes and sign of ΔG in this study for both All DC4 and BDT4 agree with the magnitude and signs of observed ΔG in summer of Beringer et al. (2005), Chambers and Chapin (2002), Huang et al. (2013), and Liu and Randerson (2008) as shown in Table S4. Future research on the effect that a tree species conversion has on seasonal ground heat fluxes is needed going forward. Further, while we have not considered management impacts on physical properties of the ground vegetation, mosses, litter, and soils, these likely affect G, and research here is also needed.

As for the annual ΔLST, the conversion to deciduous forests gave the largest magnitude change among all three management scenarios and was negative, owed mostly to its positive year-round $\Delta\alpha$, a positive λTr in summer, and a positive ΔG in spring, autumn, and winter (Figure 4). This agrees with findings by Rydsaa et al. (2015) in which evergreen forests were replaced by broadleaved forests along the southern border of boreal forests in Fennoscandia, which led to a lower LAI, higher albedo, and lower surface fluxes (sensible heat was much lower than latent heat), resulting in less heating of the boundary layer and lower near-surface temperatures and atmospheric moisture. While the annual ΔLST due to the conversion of PRESENT to highly developed forests was also negative, the magnitude of this reduction—owed mostly to increases to λTr in spring and summer—was only 25% of that associated with the deciduous conversion scenario (Table 2). Unlike in the deciduous conversion scenario, the annual ΔLST signal from $\Delta\alpha$ in the DC1-PRESENT and DC4-PRESENT scenarios was low given that the largest changes were confined to winter months (Figure 2) when available energy at the surface was low.

We find the magnitude of the simulated surface energy flux changes to be on the order approaching that which may be associated with anthropogenic land use or land cover changes (Alkama & Cescatti, 2016; Ahlswede & Thomas, 2017; Bright et al., 2017) or vegetation "greening" in the same region (Forzieri et al., 2017), reinforcing the notion that forestry is an often overlooked driver of regional energy and moisture budgets in climate modeling studies (Nabel et al., 2019; Naudts et al., 2016; Pongratz et al., 2018; Shevliakova et al., 2009; Yue et al., 2017).

The second objective of this study was to assess the relative importance of surface energy flux changes to local LST change in Nordic Fennoscandia (local being the area affected in each land model grid cell). Annually and regionally, the TDM analysis revealed that $\Delta\lambda Tr$ is the dominant signal determining the sign of the ΔLST response when converting from PRESENT to undeveloped and fully developed forests. When converting evergreen needleleaved forests to broadleaved deciduous forests, ΔH was the dominant ΔLST signal, but the combined signals from $\Delta\lambda Tr$, ΔG, and $\Delta\alpha$ determined the overall sign of the ΔLST response. The annual ΔLST was lower in the deciduous conversion scenario than in the fully developed conversion scenario irrespective of the decrease in LAI. The study by Ahlswede and Thomas (2017) in eastern North America highlights that $\Delta\alpha$ alone can contribute to ΔLST by changing the intensity of forest management

through its effect on LAI. Seasonally, $\Delta\lambda Tr$ and ΔH dominate ΔLST in the undeveloped and fully developed conversion scenarios, respectively, whereas $\Delta\alpha$ dominates in summer and ΔG in winter for the deciduous conversion scenario. The importance of $\Delta\alpha$ to ΔLST in deciduous forests is highlighted in this study primarily in summer and secondarily in other seasons. Interestingly, for the deciduous conversion scenario, seasonal signals from ΔG were larger than the other scenarios and nearly dominated ΔLST in autumn and early winter (Figure 4). However, given the lack of observational evidence and other modeling studies in the region, it is difficult to evaluate the robustness of this finding, warranting further investigation on the contribution of ΔG to ΔLST in future research. The ΔH signal dominates ΔLST during autumn and spring in all three conversion scenarios, a period when differences in both surface albedo and the latent heat of transpiration flux between the PRESENT and three scenarios are minor.

The third objective of this study was to identify management strategies leading to desirable surface energy balance outcomes in Nordic Fennoscandia. Using ΔLST as the measure, the conversion of coniferous-dominant (i.e., PRESENT) to more deciduous broadleaved forests in most parts of the region would be beneficial to surface energy balance over the longer term as judged from the annual mean ΔLST result (Figure S14). This is because in spring, autumn, and winter, these regions were found to have cooling benefits owed to increased albedo and ground heat (Figure S14). The exception is in small regions of southern Finland and Sweden, where changes to G were negative, which, when combined with the warming due to decreases to H, could not be countered by the increases to surface albedo. Increasing the proportion of older-aged forests in the region—as would be associated with decreases to regional harvesting intensities (i.e., DC4-PRESENT)—would provide annual cooling in large parts of the region. Exceptions are in northern Finland and Sweden and central and southern Norway, where there is a net annual warming due to combined effects of decreases to surface albedo, ground heat, and evaporation. Increasing the proportion of undeveloped forests in the region—as would be associated with an increase to regional harvesting intensities—would provide no cooling benefits with the exception of the small highland regions of central Norway and in the northeastern parts of the domain, where the annual mean cooling from increases to surface albedo and evaporation is greater than the warming from decreases to transpiration and H.

This study also revealed that although variations in the climate background can affect the sign and magnitude of surface fluxes (Li et al., 2016), we found little sensitivity of turbulent heat flux partitioning to interannual variability in summertime VPD (wet vs. dry environmental conditions; Figure S9).

It is important to note that our findings are based on simulations carried out offline using prescribed atmospheric forcing, thus ignoring potential atmospheric feedbacks. For instance, despite the different geographic region, Ahlswede and Thomas (2017**)** showed that ΔLAI resulted in a reduced cloud cover, which in turn impacted the surface energy balance. Vanden Broucke et al. (2015) presented a new methodology for evaluating biogeophysical impacts of land use change in a regional climate model in coupled mode but acknowledged that the offline model simulations are necessary and useful because they remove a potential source of error produced by atmospheric model (in coupled mode) and make longer simulations possible (Demuzere et al., 2013). The study by Rydsaa et al. (2015) used a coupled model to evaluate the sensitivity of regional climate in Fennoscandia to changes in vegetation structure. Both experiments in Rydsaa et al. (2015) mimic our All DC4 and BDT4 scenarios. The evergreen forest expansion (Experiment 1, higher LAI) led to decreases in albedo and increases in the latent heat flux, which subsequently led to a deeper and wetter planetary boundary layer. Increased summer precipitation and increased roughness length and aerodynamic conductance lowered sensible heat flux, causing a lowering Bowen ratio. Our offline study can be directly compared to all DC4 scenarios, where higher LAI of forest led to lower Bowen ratio, decreased albedo, lower sensible heat, and higher latent heat flux. Further, replacement of conifers with deciduous forest (Experiment 2, species change) led to higher albedo and lower surface fluxes (H much lower than LE). BDT4 of our offline scenario also led to higher albedo, lower sensible heat, but higher latent heat flux.

Another study by Thackeray et al. (2019) used an offline and a coupled modeling framework to determine the influence of perturbation to surface albedo (surface energy balance) on climate (near-surface temperature). From Figure 1 of their study, it appears that the spatial patterns, signs, and magnitudes of the near-surface temperature response over boreal forest regions do not differ much between their offline and coupled simulations, particularly for winter. In Nordic Fennoscandia, in particular, atmospheric

feedbacks are likely negligible relative to the first-order surface energy balance response at the scale and pattern of current and future regional forestry activities (Chen & Dirmeyer, 2020; Laguë et al., 2019).

In this study, we quantitatively assessed the sensitivity of surface energy and water fluxes to changes to forest structure and composition across space and time in Nordic Fennoscandia (Norway, Sweden, and Finland) and found that these can be equally as sensitive to forest management activities like harvesting and species conversion as to other forms of anthropogenic land disturbances (i.e., land cover/land use changes). Results from our high spatial resolution study can guide or help inform regional resource managers about the consequences of increasing harvest intensities (e.g., results of DC1-PRESENT) or about the longer-term consequences of tree species conversion (BDT4-PRESENT) as they affect surface energy and moisture budgets and LST.

Data Availability Statement

The data of enhanced classification of forests in Fennoscandia can be accessed at https://doi.org/10.5194/bg-15-399-2018, (2018).

Acknowledgments
We acknowledge modeling support from Hui Tang and Ronny Meier for the code of separate soils columns per PFT in CLM4.5.

References

Ahlswede, B. J., & Thomas, R. Q. (2017). Community Earth System Model simulations reveal the relative importance of afforestation and forest management to surface temperature in eastern North America. *Forests*, *8*(12), 1, 499–10. https://doi.org/10.3390/f8120499

Alibakhshi, S., Naimi, B., Hovi, A., Crowther, T. W., & Rautiainen, M. (2020). Quantitative analysis of the links between forest structure and land surface albedo on a global scale. *Remote Sensing of Environment*, *246*, 111854. https://doi.org/10.1016/j.rse.2020.111854

Alkama, R., & Cescatti, A. (2016). Biophysical climate impacts of recent changes in global forest cover. *Science*, *351*(6273), 600–604. https://doi.org/10.1126/science.aac8083

Anderson, R. G., Canadell, J. G., Randerson, J. T., Jackson, R. B., Hungate, B. A., Baldocchi, D. D., et al. (2011). Biophysical considerations in forestry for climate protection. *Frontiers in Ecology and the Environment*, *9*(3), 174–182. https://doi.org/10.1890/090179

Beringer, J., Chapin, F. S., Thompson, C. C., & McGuire, A. D. (2005). Surface energy exchanges along a tundra-forest transition and feedbacks to climate. *Agricultural and Forest Meteorology*, *131*(3–4), 143–161. https://doi.org/10.1016/j.agrformet.2005.05.006

Betts, R. A. (2000). Offset of the potential carbon sink from boreal forestation by decreases in surface albedo. *Nature*, *408*(6809), 187–190. https://doi.org/10.1038/35041545

Betts, R. A., Falloon, P. D., Goldewijk, K. K., & Ramankutty, N. (2007). Biogeophysical effects of land use on climate: Model simulations of radiative forcing and large-scale temperature change. *Agricultural and Forest Meteorology*, *142*(2–4), 216–233. https://doi.org/10.1016/j.agrformet.2006.08.021

Bohn, F. J., May, F., & Huth, A. (2018). Species composition and forest structure explain the temperature sensitivity patterns of productivity in temperate forests. *Biogeosciences*, *15*(6), 1795–1813. https://doi.org/10.5194/bg-15-1795-2018

Bonan, G. B. (1993). Importance of leaf area index and forest type when estimating photosynthesis in boreal forests. *Remote Sensing of Environment*, *43*(3), 303–314. https://doi.org/10.1016/0034-4257(93)90072-6

Bonan, G. B. (2008). Forests and climate change: Forcings, feedbacks, and the climate benefits of forests. *Science*, *320*(5882), 1444–1449. https://doi.org/10.1126/science.1155121

Bright, R. M., Davin, E., O'Halloran, T., Pongratz, J., Zhao, K., & Cescatti, A. (2017). Local temperature response to land cover and management change driven by non-radiative processes. *Nature Climate Change*, *7*(4), 296–302. https://doi.org/10.1038/nclimate3250

Bright, R. M., Eisner, S., Lund, M. T., Majasalmi, T., Myhre, G., & Astrup, R. (2018). Inferring surface albedo prediction error linked to forest structure at high latitudes. *Journal of Geophysical Research: Atmospheres*, *123*, 4910–4925. https://doi.org/10.1029/2018JD028293

Bright, R. M., Zhao, K., Jackson, R. B., & Cherubini, F. (2015). Quantifying surface albedo and other direct biogeophysical climate forcings of forestry activities. *Global Change Biology*, *21*(9), 3246–3266. https://doi.org/10.1111/gcb.12951

Burakowski, E., Tawfik, A., Ouimette, A., Lepine, L., Novick, K., Ollinger, S., et al. (2018). The role of surface roughness, albedo, and Bowen ratio on ecosystem energy balance in the Eastern United States. *Agricultural and Forest Meteorology*, *249*(October 2017), 367–376. https://doi.org/10.1016/j.agrformet.2017.11.030

Chambers, S. D. (2005). Fire effects on net radiation and energy partitioning: Contrasting responses of tundra and boreal forest ecosystems. *Journal of Geophysical Research*, *110*, D09106. https://doi.org/10.1029/2004JD005299

Chambers, S. D., & Chapin, F. S. (2002). Fire effects on surface-atmosphere energy exchange in Alaskan black spruce ecosystems: Implications for feedbacks to regional climate. *Journal of Geophysical Research*, *108*(D1), 8145. https://doi.org/10.1029/2001JD000530

Chen, L., & Dirmeyer, P. A. (2016). Adapting observationally based metrics of biogeophysical feedbacks from land cover/land use change to climate modeling. *Environmental Research Letters*, *11*, 034002. https://doi.org/10.1088/1748-9326/11/3/034002

Chen, L., & Dirmeyer, P. A. (2020). Reconciling the disagreement between observed and simulated temperature responses to deforestation. *Nature Communications*, *11*, 202. https://doi.org/10.1038/s41467-019-14017-0

da Rocha, H. R., Goulden, M. L., Miller, S. D., Menton, M. C., Pinto, L. D. V. O., de Freitas, H. C., e Silva Figueira, A. M. (2004). Seasonality of water and heat fluxes over a tropical forest in eastern Amazonia. *Ecological Applications*, *14*(sp4), 22–32. https://doi.org/10.1890/02-6001

Demuzere, M., Oleson, K., Coutts, A. M., Pigeon, G., & van Lipzig, N. P. M. (2013). Simulating the surface energy balance over two contrasting urban environments using the Community Land Model Urban. *International Journal of Climatology*, *33*(15), 3182–3205. https://doi.org/10.1002/joc.3656

Dixon, A. K. R. (1976). Analysis of seasonal leaf fall in north temperate deciduous forests. Oikos, *27*(2), 300–306, DOI: https://doi.org/10.2307/3543909

Eugster, W., Rouse, W. R., Pielke Sr, R. A., Mcfadden, J. P., Baldocchi, D. D., Kittel, T. G. F, et al. (2000). Land-atmosphere energy exchange in Arctic tundra and boreal forest: available data and feedbacks to climate. *Global Change Biology*, *6*(S1), 84–115. https://doi.org/10.1046/j.1365-2486.2000.06015.x

Fisher, R. A., Muszala, S., Verteinstein, M., Lawrence, P., Xu, C., McDowell, N. G., et al. (2015). Taking off the training wheels: The properties of a dynamic vegetation model without climate envelopes, CLM4.5(ED). *Geoscientific Model Development*, *8*(11), 3593–3619. https://doi.org/10.5194/gmd-8-3593-2015

Forzieri, G., Alkama, R., Miralles, D. G., & Cescatti, A. (2017). Satellites reveal contrasting responses of regional climate to the widespread greening of Earth. *Science*, *356*(6343), 1180–1184. https://doi.org/10.1126/science.aal1727

Hovi, A., Liang, J., Korhonen, L., Kobayashi, H., & Rautiainen, M. (2016). Quantifying the missing link between forest albedo and productivity in the boreal zone. *Biogeosciences*, *13*(21), 6015–6030. https://doi.org/10.5194/bg-13-6015-2016

Huang, S., Dahal, D., Singh, R., Liu, H., Young, C., & Liu, S. (2013). Spatially explicit surface energy budget and partitioning with remote sensing and flux measurements in a boreal region of Interior Alaska. *Theoretical and Applied Climatology*, *113*(3–4), 549–560. https://doi.org/10.1007/s00704-012-0806-8

Jackson, R. B., Randerson, J. T., Canadell, J. G., Anderson, R. G., Avissar, R., Baldocchi, D. D., et al. (2008). Protecting climate with forests. *Environmental Research Letters*, *3*, 044006. https://doi.org/10.1088/1748-9326/3/4/044006

Juang, J.-Y., Katul, G., Siqueira, M., Stoy, P., & Novick, K. (2007). Separating the effects of albedo from eco-physiological changes on surface temperature along a successional chronosequence in the southeastern United States. *Geophysical Research Letters*, *34*, L21408. https://doi.org/10.1029/2007GL031296

Kuusinen, N., Stenberg, P., Korhonen, L., Rautiainen, M., & Tomppo, E. (2016). Structural factors driving boreal forest albedo in Finland. *Remote Sensing of Environment*, *175*, 43–51. https://doi.org/10.1016/j.rse.2015.12.035

Laguë, M. M., Bonan, G. B., & Swann, A. L. S. (2019). Separating the impact of individual land surface properties on the terrestrial surface energy budget in both the coupled and uncoupled land–atmosphere system. *Journal of Climate*, *32*(18), 5725–5744. https://doi.org/10.1175/JCLI-D-18-0812.1

Launiainen, S., Katul, G. G., Kolari, P., Lindroth, A., Lohila, A., Aurela, M., et al. (2016). Do the energy fluxes and surface conductance of boreal coniferous forests in Europe scale with leaf area? *Global Change Biology*, *22*(12), 4096–4113. https://doi.org/10.1111/gcb.13497

Lawrence, D. M., Fisher, R. A., Koven, C. D., Oleson, K. W., Swenson, S. C., Bonan, G., et al. (2019). The Community Land Model version 5: Description of new features, benchmarking, and impact of forcing uncertainty. *Journal of Advances in Modeling Earth Systems*, *11*(12), 4245–4287. https://doi.org/10.1029/2018MS001583

Lee, X., Goulden, M. L., Hollinger, D. Y., Barr, A., Black, T. A., Bohrer, G., et al. (2011). Observed increase in local cooling effect of deforestation at higher latitudes. *Nature*, *479*(7373), 384–387. https://doi.org/10.1038/nature10588

Li, Y., De Noblet-Ducoudré, N., Davin, E. L., Motesharrei, S., Zeng, N., Li, S., & Kalnay, E. (2016). The role of spatial scale and background climate in the latitudinal temperature response to deforestation. *Earth System Dynamics*, *7*(1), 167–181. https://doi.org/10.5194/esd-7-167-2016

Li, Y., Zhao, M., Motesharrei, S., Mu, Q., Kalnay, E., & Li, S. (2015). Local cooling and warming effects of forests based on satellite observations. *Nature Communications*, *6*(1), 6603–6608. https://doi.org/10.1038/ncomms7603

Liu, H., & Randerson, J. T. (2008). Interannual variability of surface energy exchange depends on stand age in a boreal forest fire chronosequence. *Journal of Geophysical Research*, *113*, 1, G01006–13. https://doi.org/10.1029/2007JG000483

Lukeš, P., Stenberg, P., & Rautiainen, M. (2013). Relationship between forest density and albedo in the boreal zone. *Ecological Modelling*, *261-262*, 74–79. https://doi.org/10.1016/j.ecolmodel.2013.04.009

Lussana, C., Tveito, O. E., & Uboldi, F. (2018). Three-dimensional spatial interpolation of 2 m temperature over Norway. *Quarterly Journal of the Royal Meteorological Society*, *144*(711), 344–364. https://doi.org/10.1002/qj.3208

Luyssaert, S., Jammet, M., Stoy, P. C., Estel, S., Pongratz, J., Ceschia, E., et al. (2014). Land management and land-cover change have impacts of similar magnitude on surface temperature. *Nature Climate Change*, *4*(5), 389–393. https://doi.org/10.1038/nclimate2196

Luyssaert, S., Marie, G., Valade, A., Chen, Y. Y., Njakou Djomo, S., Ryder, J., et al. (2018). Trade-offs in using European forests to meet climate objectives. *Nature*, *562*(7726), 259–262. https://doi.org/10.1038/s41586-018-0577-1

Majasalmi, T., Eisner, S., Astrup, R., Fridman, J., & Bright, R. M. (2018). An enhanced forest classification scheme for modeling vegetation–climate interactions based on national forest inventory data. *Biogeosciences*, *15*(2), 399–412. https://doi.org/10.5194/bg-15-399-2018

Meier, R., Davin, E. L., Lejeune, Q., Hauser, M., Li, Y., Martens, B., et al. (2018). Evaluating and improving the Community Land Model's sensitivity to land cover. *Biogeosciences*, *15*(15), 4731–4757. https://doi.org/10.5194/bg-15-4731-2018

Nabel, J. E. M. S., Naudts, K., & Pongratz, J. (2019). Accounting for forest age in the tile-based dynamic global vegetation model JSBACH4 (4.20p7; git feature/forests)—A land surface model for the ICON-ESM. *Geoscientific Model Development Discussion*, *20*, 1–24. https://doi.org/10.5194/gmd-2019-68

Naudts, K., Chen, Y., McGrath, M. J., Ryder, J., Valade, A., Otto, J., & Luyssaert, S. (2016). Forest management: Europe's forest management did not mitigate climate warming. *Science*, *351*(6273), 597–600. https://doi.org/10.1126/science.aad7270

Nobel, P. S., & Geller, G. N. (1987). Temperature modelling of wet and dry desert soils. *Journal of Ecology*, *75*(1), 247–258. https://doi.org/10.2307/2260549

Oleson, K. W., Lawrence, D. M., Bonan, G. B., Drewniak, B., Huang, M., Koven, C. D., et al. (2013). Technical description of version 4. 5 of the Community Land Model (CLM). *NCAR Technical Note*, (April).

Olsson, C., & Jönsson, A. M. (2014). Process-based models not always better than empirical models for simulating budburst of Norway spruce and birch in Europe. *Global Change Biology*, *20*(11), 3492–3507. https://doi.org/10.1111/gcb.12593

Oyeyemi, K. D., Sanuade, O. A., Oladunjoye, M. A., Aizebeokhai, A. P., Olaojo, A. A., Fatoba, J. O., et al. (2018). Data on the thermal properties of soil and its moisture content. *Data in Brief*, *17*, 900–906. https://doi.org/10.1016/j.dib.2018.02.018

Pongratz, J., Dolman, H., Don, A., Erb, K. H., Fuchs, R., Herold, M., et al. (2018). Models meet data: Challenges and opportunities in implementing land management in Earth system models. *Global Change Biology*, *24*, 1470–1487. https://doi.org/10.1111/gcb.13988

Rigden, A. J., & Li, D. (2017). Attribution of surface temperature anomalies induced by land use and land cover changes. *Geophysical Research Letters*, *44*, 6814–6822. https://doi.org/10.1002/2017GL073811

Rydsaa, J. H., Stordal, F., & Tallaksen, L. M. (2015). Sensitivity of the regional European boreal climate to changes in surface properties resulting from structural vegetation perturbations. *Biogeosciences*, *12*(10), 3071–3087. https://doi.org/10.5194/bg-12-3071-2015

Sato, H., Ito, A., Ito, A., Ise, T., & Kato, E. (2015). Current status and future of land surface models. *Soil Science and Plant Nutrition*, *61*(1), 34–47. https://doi.org/10.1080/00380768.2014.917593

Schultz, N. M., Lee, X., Lawrence, P. J., Lawrence, D. M., & Zhao, L. (2016). Assessing the use of subgrid land model output to study impacts of land cover change. *Journal of Geophysical Research: Atmospheres*, *121*, 6133–6147. https://doi.org/10.1002/2016JD025094

Schulz, J., & Vogel, G. (2020). Improving the processes in the land surface scheme TERRA: Bare soil evaporation and skin temperature. *Atmosphere*, *11*, 513. https://doi.org/10.3390/atmos11050513

Shevliakova, E., Pacala, S. W., Malyshev, S., Hurtt, G. C., Milly, P. C. D., Caspersen, J. P., et al. (2009). Carbon cycling under 300 years of land use change: Importance of the secondary vegetation sink. *Global Biogeochemical Cycles*, *23*, GB2022. https://doi.org/10.1029/2007GB003176

Thackeray, C. W., Fletcher, C. G., & Derksen, C. (2019). Diagnosing the impacts of Northern Hemisphere surface albedo biases on simulated climate. *Journal of Climate*, *32*(6), 1777–1795. https://doi.org/10.1175/JCLI-D-18-0083.1

Vanden Broucke, S., Luyssaert, S., Davin, E. L., Janssens, I., & van Lipzig, N. (2015). New insights in the capability of climate models to simulate the impact of LUC based on temperature decomposition of paired site observations. *Journal of Geophysical Research: Atmospheres*, *120*, 5417–5436. https://doi.org/10.1002/2015JD023095

Winckler, J., Reick, C. H., Bright, R. M., & Pongratz, J. (2019). Importance of surface roughness for the local biogeophysical effects of deforestation. *Journal of Geophysical Research: Atmospheres*, *124*, 8605–8618. https://doi.org/10.1029/2018jd030127

Yue, C., Ciais, P., Luyssaert, S., Li, W., McGrath, M. J., Chang, J., & Peng, S. (2017). Representing anthropogenic gross land use change, wood harvest and forest age dynamics in a global vegetation model ORCHIDEE-MICT (r4259). *Geoscientific Model Development Discussion*, *8*, 317–340. https://doi.org/10.5194/gmd-2017-118

Zeng, X., Shajkh, M., Dai, Y., Dickinson, R. E., & Myneni, R. (2002). Coupling of the Common Land Model to the NCAR Community Climate Model. *Journal of Climate*, *15*(14), 1832–1854. https://doi.org/10.1175/1520-0442(2002)015<1832:COTCLM%3E2.0.CO;2

Zhao, K., & Jackson, R. B. (2014). Biophysical forcings of land-use changes from potential forestry activities in North America. *Ecological Monographs*, *84*(2), 329–353. https://doi.org/10.1890/12-1705.1